SERI/TP-212-2355
UC Category: 63
DE84013001

Glow Discharge Amorphous Silicon Tin Alloys

A. H. Mahan
A. Sanchez
D. L. Williamson
B. von Roedern
A. Madan

June 1984

Presented at the 17th IEEE
Photovoltaics Specialists Conference
Kissimmee, Florida
1-5 May 1984

Prepared under Task No. 3423.10
FTP No. 461

Solar Energy Research Institute
A Division of Midwest Research Institute

1617 Cole Boulevard
Golden, Colorado 80401

Prepared for the
U.S. Department of Energy
Contract No. DE-AC02-83CH10093

Printed in the United States of America
Available from:
National Technical Information Service
U.S. Department of Commerce
5285 Port Royal Road
Springfield, VA 22161
Price:
Microfiche A01
Printed Copy A02

NOTICE

This report was prepared as an account of work sponsored by the United States Government. Neither the United States nor the United States Department of Energy, nor any of their employees, nor any of their contractors, subcontractors, or their employees, makes any warranty, express or implied, or assumes any legal liability or responsibility for the accuracy, completeness or usefulness of any information, apparatus, product or process disclosed, or represents that its use would not infringe privately owned rights.

GLOW DISCHARGE AMORPHOUS SILICON TIN ALLOYS

A.H. Mahan, A. Sanchez*, D.L. Williamson†, B. von Roedern, and A. Madan

Solar Energy Research Institute, Golden, CO
*CIUDAD Universitaria, Mexico
†Colorado School of Mines, Golden, CO

Abstract

We present basic density of states, photoresponse, and transport measurements made on low bandgap a-SiSn:H alloys produced by RF glow discharge deposition of SiH_4, H_2 and $Sn(CH_3)_4$. Although we demonstrate major changes in the local bonding structure and the density of states, the normalized photoresponse still remains poor. We provide evidence that two types of defect levels are produced with Sn alloying, and that the resultant density of states increase explains not only the n- to p-type conductivity transition reported earlier, but also the photoresponse behavior. We also report that a-SiSn:H can be doped with P. From our device analysis we suggest that in order to improve the alloy performance significantly, the density of states should be decreased to levels comparable to or lower than those presently obtained in a-Si:H.

Introduction

Hydrogenated amorphous silicon based alloys are of considerable interest regarding applications in multijunction thin film solar cells (1). Much work has been reported on a-SiGe:H as a potential low bandgap material (2-4) and recently, several studies on a-SiSn:H have also been reported (1,5-7). However, the electronic properties of both the systems generally degrade with alloying. In particular, alloy materials with a significant bandgap shift relative to amorphous silicon show an increase in the density of localized states [g(E)] as well as a decrease in the photoresponse. It has been suggested (8) that the increase in g(E) with alloying, especially for a-SiGe:H, arises in part from the preferential attachment (PA) of the dangling bond terminator (H) to Si. The decrease in photoconductivity may be due not only to the g(E) increase but also to a change in the local bonding structure of the material, from predominantly Si-H bonding, in a-Si:H, to multiply bonded H in the alloys (SiH_2, GeH_2) (9). The commonality of the local bonding trends and an increase in the g(E) when Si is alloyed with Ge, Sn, and C has been noted in a recent paper (6); it was suggested that in these alloys a similar type of defect is created near the valence band edge, E_v; this also explains the n- to p-type transition observed in a SiSn:H, and the trend towards p-type behavior that seems to exist when a-Si:H is alloyed with Ge or C.

In this paper we provide some evidence that two types of defect levels are produced with alloying, and that the resultant increase in g(E) explains not only the n- to p- type conductivity transition reported earlier, but also the drastic decrease in photoresponse. Further, we report that a-SiSn:H can be doped with P and shows a significant change in the dark conductivity. From our device analysis we suggest that in order to improve the alloy performance significantly, g(E) should be decreased to levels comparable to or even lower than those presently obtained in a-Si:H.

Experimental Results

The a-SiSn:H films discussed in the present study were deposited in an RF glow discharge apparatus using SiH_4, H_2 and $Sn(CH_3)_4$ gas mixtures. The details of the experimental apparatus are given elsewhere (6). Typical deposition parameters were 260°C substrate temperature, 300-600 mT chamber pressure, 0.17-0.33W/cm^2 RF power density, and 4-30 sccm total gas flow rates.

Two experimental techniques have been used to measure the g(E) in a-SiSn:H. In the first type of measurement, the space charge limited current (SCLC) technique (10) was performed for films deposited in a n^+-i-n^+ configuration, yielding state densities above the Fermi level E_F. In the second type of measurement, subbandgap absorption was measured on films deposited on quartz by the photothermal deflection spectroscopy technique (PDS) (11). In order to probe the nature of the localized states produced by alloying, we have examined samples with small Sn content. This was done because any structure that might be observed by SCLC or PDS tends to be smeared out for larger Sn contents. An example of the raw data for low and high Sn alloy contents is shown in Fig. 1, along with representative data for a-Si:H.

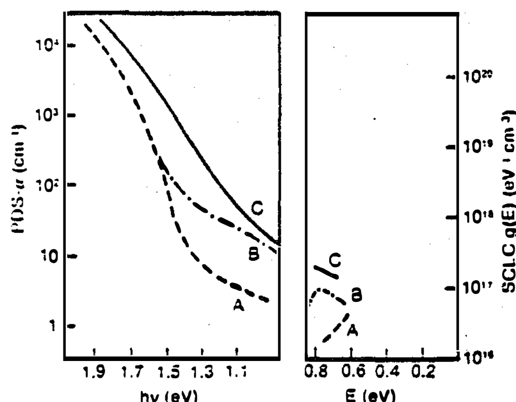

Figure 1 - PDS absorption coefficient (α) versus excitation energy (hν), and SCLC g(E) versus energy (E) for A: a-Si:H; B: a-SiSn:H low alloy regime (2 at. % Sn); and C: a-SiSn:H high alloy regime (10 at. % Sn).

We attribute the initial g(E) structure (using SCLC technique) observed at small Sn concentrations to an increase in the dangling bond defect density. From the conductivity activation energy measurements on these samples, this structure is found to be located near or slightly above the midgap position. Support for this interpretation is provided by an increase in the dangling bond density for both Ge and C alloying, (12,13) and measurements on intrinsic a-Si:H which have located the Si dangling bond defect near the midgap position (14).

In order to correlate the absorption coefficient, α, derived from the PDS data with g(E), we have used the following calibration procedure. Nielson et. al. (15) have reported photoemission results showing that heavy P doping of a-Si:H creates an excess g(E) located approximately 0.4eV above E_v (or 1.3 to 1.4eV below E_c), with a peak value of 5 x 10^{19} eV^{-1} cm^{-3}. The width (FWHM) of this excess g(E) is approximately 0.5eV. PDS measurements (16) on heavily P doped a-Si:H have enabled a correlation of α=1cm^{-1} with g(E) = 10^{17} eV^{-1} cm^{-3}.

Table I shows optical, conductivity, and g(E) parameters for representative a-SiSn:H films prepared under different deposition conditions. The table is divided into three series in order to demonstrate several trends in sample behavior, and includes one a-Si:H sample for comparison purposes. Films in series I were deposited at high flow rate conditions, with only a variation in the $Sn(CH_3)_4$ gas flow. In series II, films of constant bandgap E_g are presented as a function of decreasing gas flow rate. Finally, series III presents films deposited as a function of increasing RF power. It should be noted that although the films presented in the table show some photoresponse improvement with changes in deposition parameters ((σ_L/σ_D) changes by several orders of magnitude with σ_L measured at AM1 light intensity), the normalized $\eta\mu\tau$ photoresponse remains small (where η is the quantum efficiency, μ is the mobility and τ is the recombination lifetime); therefore, the discussion will focus on changes in the local bonding structure, and how these correlate with g(E) measurements.

In Series I, high g(E) values measured both by SCLC and PDS techniques are accompanied by relatively high Sn and C contents and infrared absorption (IR) modes indicating H multiply bonded to both C (2900cm^{-1} mode indicating CH_n vibrations) and Si (2100, 845-890cm^{-1} modes indicating SiH_2 polymerization). Both types of IR modes have been previously identified in a-SiC:H films which exhibit poor photoresponse (17). That work also demonstrated that inclusion of C accentuates the creation of SiH_2 polymer complexes as well as an increase in dangling bond density.

In Series II, films of constant E_g exhibit a reduced alloy (Sn,C) content and a reduction in CH_n bonding with reduced gas flow rate. This change in local bonding enables H to passivate an increasing number of dangling bonds associated with either Si or Sn. Accordingly, we see a significant decrease in the g(E) from SCLC measurements and some decrease in the g(E) as derived from PDS measurements.

Finally, in Series III, a further reduction in the g(E) from PDS measurements is achieved at higher RF power levels, and is accompanied by the virtual elimination of the SiH_2 polymer signature (i.e., 2100cm^{-1} mode and its corresponding 845-890cm^{-1} doublet). It is possible, therefore, that the g(E) defect below midgap can be associated in part with SiH_2 local bonding in the alloy. It should be noted that the amount of H now singly bonded to Si, as evidenced by the 2000cm^{-1} peak, has increased dramatically. This is consistent with an increased passivation of dangling bonds by H when the multiply bonded H in the film is reduced. In these samples, SCLC and activation energy measurements indicate that E_f is situated in a region of decreasing g(E), and therefore the minimum g(E) may be lower than the SCLC derived g(E) values quoted in the table.

It is worth noting that an alternative explanation for the origin of the g(E) defect below midgap can also be advanced. In spite of the changes, and apparent improvements in the local bonding structure, the PA ratio of H to Si versus Sn remains high. This suggests the existence of a sizeable defect density associated directly with Sn incorporation. Support for this interpretation is provided by the suggestion (18) of a localized state created near E_v by the addition of Sn to thermally evaporated a-Si, and the identical conductivity behavior (n- to p-type conductivity transiton) previously noted using different Sn source gases ($Sn(CH_3)_4$, $SnCl_4$) (6).

Although considerable improvement has been made in altering the local bonding structure and

TABLE 1

	Deposition Cond.			EPMA		IR				g(E)			Conductivity			
Sample	Power Watt	Flow* SCCM	Pr. mTorr	Sn at%	C at%	Si-H# %	C-Hx %	PA^{Sn}_{Si} —	SiH_2 —	SCLC+	α_{PDS}¢ cm^{-1}	PDS+	σ_D $(\Omega cm)^{-1}$	σ_L/σ_D —	$\eta\mu\tau$ cm^2V^{-1}	E_g eV
Feb 10/1	5	32(0)	600	—	—	6.0			No	1E16	4	4E17	2E-9	250000	7E-6	1.75
Feb 10/2	5	32(15)	600	8.0	2.2	9.5	2.8	1/4.5	Yes				7E-10	3.1	3E-11	1.65
Feb 10/3	5	32(20)	600	9.4	2.9	9.6	3.2	1/5.7	Yes	8E17	375	4E19	4E-9	1.5	2E-11	1.61
Feb 13/1	5	32(30)	600	14.5	3.3	9.1	6.7		Yes	9E17			6E-8	1.1	1E-10	1.50
Feb 10/3	5	32(20)	600	9.4	2.9	9.6	3.2	1/5.7	Yes	8E17	375	4E19	4E-9	1.5	2E-11	1.61
Mar 2/1	5	16(10)	600	8.8	1.7	11.6	2.1	1/6.3	Yes	3E17	130	1E19	2E-11	30	2E-11	1.59
Mar 8/1	5	4(5)	600	6.4	1.5	11.0	1.3	1/5.6	Yes	1.5E17	220	2E19	2E-11	56	5E-11	1.60
Mar 15/2	2.5	4(2)	300	7.7	2.0	7.2	2.1	1/2.7	Yes	5E17	150	1.5E19	3E-11	31	1E-11	1.64
Mar 14/2	7.5	4(2)	300	5.7	1.2	12.4	0.6	1/9.6	No	2E17	100	1E19	4E-12	500	5E-11	1.55
Mar 15/1	10	4(2)	300	4.7	1.3	18.5	0.5	1/10.2	No	1.5E17	30	3E18	5E-12	180	2E-11	1.51
Mar 21/1	15	4(2)	300	4.5	1.4	16.6	—	1/10.5	No	1.5E17		—	2E-11	43	3E-11	1.51

* The numbers in parenthesis represent Sn flows as measured on a Matheson 610 Rotameter scale, from 0–100.

\# The area under the 2000–2100cm^{-1} peak enabled these values to be obtained.

x The area under the 2900cm^{-1} peak enabled these values to be obtained.

\+ The units are $(cm^3 eV)^{-1}$.

¢ The α_{PDS} values are measured at an excitation energy .5eV below E_g.

reducing g(E) in a-SiSn:H, both near and below midgap, g(E) remains significantly higher than in a-Si:H, and the normalized photoresponse remains poor. Figure 2 shows a model for g(E) explaining this behavior. In particular, we identify two different types of defects associated with the addition of Sn, the neutral dangling bond located near midgap (as probed by SCLC), and a second defect level located below midgap (as probed by PDS) which seems to be enhanced whenever SiH_2 polymer complexes are present. The trends in deposition conditions which reduce the magnitudes of these levels are indicated. In these alloys the ratio of below midgap to midgap density of states $(g(E_v + 0.4)/g(E_f))$ has increased a factor of 10 compared to a-Si:H (19). This is consistent with E_f shifting to below midgap and a switch to p-type dark transport with increasing Sn incorporation; this will occur if some of the below midgap states act as acceptor levels. It is possible to explain the decrease of the $\mu\tau$ products in terms of changes in activation energy, ΔE. In particular, Kirby et al. (20) have shown that the $\mu\tau$ products depend on the position of E_f or on the charged nature of the midgap states. In a-SiSn:H, the decrease in $(\mu\tau)_e$ could be due to a shift of E_f away from the conduction band, while the small $(\mu\tau)_h$ is caused by an unfavorable change from extended state to hopping conduction, in which case the mobility is expected to be much lower.

In order to achieve an improved photoresponse, we have doped the a-SiSn:H with Phosphorous. Figure 3 illustrates the $\eta\mu\tau$, σ_D, and ΔE behavior of such films having E_g ~1.55eV as a function of increased P doping. A recovery of the $\eta\mu\tau$ product is noted as well as a large increase in the dark conductivity. However, the smallest ΔE obtained upon doping is 0.42eV, which is larger than that obtained in a-Si:H doped at the same level (21). This indicates less efficient doping of a-SiSn:H and is consistent with a larger DOS in this alloy.

Some Device Aspects

In the above discussion we have argued that the electronic properties of the alloys generally degrade with the inclusion of the alloying element. It is, therefore, of interest to consider the limits to the device performance when the bandgap is altered. We consider now the upper limit to the short circuit current, J_{sc}, and the open circuit voltage, V_{oc}, in an amorphous semiconductor as a function of changes in g(E) spectra. We shall assume that geminate

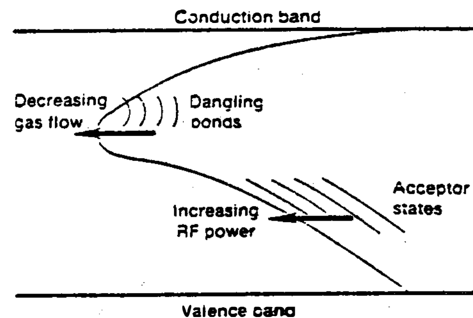

Figure 2 - A schematic representation of g(E) of a-SiSn:H, as inferred from PDS and SCLC measurements. Two types of defect levels are noted, a dangling bond state located near midgap, and an acceptor state located below midgap. The trends in deposition conditions that reduce these levels are noted.

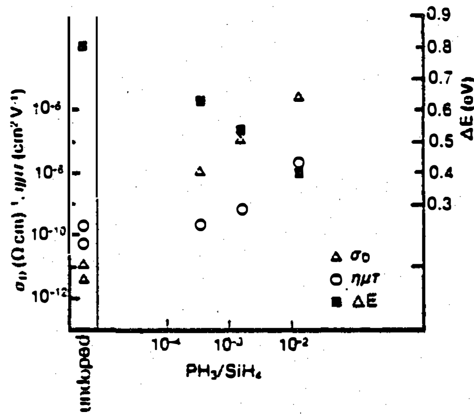

Figure 3 - Doping behavior of a-SiSn:H as a function of PH_3/SiH_4 gas ratio. The bandgaps of these films are approximately 1.55eV. The normalized photoresponse is measured at 600 nm with an incident photon flux of 3.4 x 10^{15} photons $(cm^2s)^{-1}$.

recombination is not important as seems to be the case for a-Si based alloys (22).

Using the absorption coefficient, α, and the incident power, P, as a function of wavelength, λ, the maximum short circuit current density, J_{sc} (based on collection efficiency of unity) as a function of E_g can be calculated. For ease of calculation, we approximate the AM-0 spectra to 5800K black body radiation which yields the total integrated power to be 135.7 mW cm^{-2}. The absorption coefficient can be written in terms of Tauc's Law and is given by,

$$\alpha(\lambda) = B^2 (h\nu - E_g)^2/h\nu \qquad (1)$$

where B = 700 $eV^{1/2}$ $cm^{-1/2}$ (23). In Fig. 4 , we show the J_{sc} as a function of the bandgap E_g. We calculate that for E_g = 1.7 eV, J_{sc} = 29 mA cm^{-2}. This reduces to 21.3 mA $(cm)^{-2}$ when the spectrum is normalized to an incident power of 100 mW cm^{-2}, which corresponds closely to the AM-1 incident intensity.

The value of V_{oc} can be estimated for an amorphous semiconductor if we consider that the density of states spectrum can be written in the form

$$g(E) = g_{min} \operatorname{Cosh} \{(E-E_f)/E_{ch}\} + g_o \qquad (2)$$

where the Fermi level, E_f, is assumed to be located at the mid gap position and E_{ch} is the characteristic energy which defines the slope of the conduction and valence band tails. Under uniform generation, steady state conditions, and by considering the capture and emission of electrons, one can define a trap modulated Fermi function for electrons, by

$$f(E)=(Rn/(Rn+p))[1+\exp(E-E^n_{tf})/kT]^{-1} \qquad (3)$$

where for energies $E>E^n_{tf}$ the centers act primarily as traps and for $E<E^n_{tf}$ the centers act as recombination sites. R is defined as the ratio of the rate constants for capture of electrons and holes. A similar expression can be derived for holes. Using the charge neutrality condition and recognizing that at V_{oc}, the recombination rate is equal to the generation rate, then the free carrier concentrations n and p can be found. From the resulting positions of the quasi Fermi levels E_{fn} and E_{fp}, we can deduce the open circuit voltage, V_{oc}, from $V_{oc} = E_{fn} - E_{fp}$.

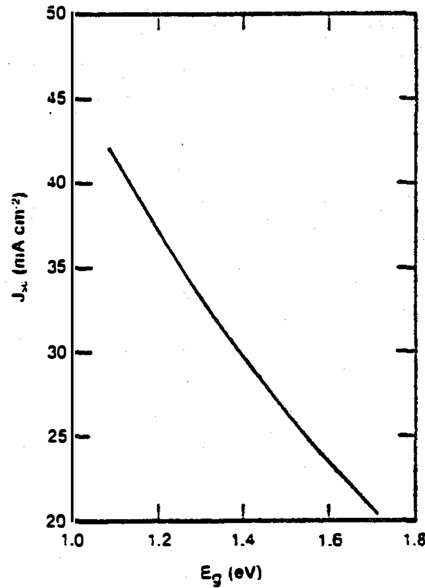

Figure 4 - Short circuit current (J_{sc}) assuming total collection, is plotted as a function of E_g for an incident illumination of 100mW cm^{-2}.

In Fig. 5, we plot V_{oc} as a function of E_g, with varying characteristic energies E_{ch} with g_o kept constant at 10^{16} cm^{-3} eV^{-1}. We should note that the value of V_{oc} falls off sharply when E_{ch} is increased. For increasingly complex alloys, we expect increased positional as well as compositional disorder, with the consequence of an increase in the width of band tails (corresponding to an increase in E_{ch}). This will increase the recombination and hence lead to a large drop in the V_{oc}. In summary, the results of Figs. 4 and 5 reveal that even if we assume total current collection, then the increase in J_{sc} with bandgap reduction is more than offset by a decrease in V_{oc}. We also conclude that, based on this model, the quest for low g_o values is perhaps not sufficient but that more attention should also be paid to the extent and width of the band tails, if alloying techniques are to succeed. In this regard, Sn may have advantages over Ge, as the alloying element since to decrease the band gap an equivalent amount, much more Ge is required than Sn. However, as is evident from the foregoing discussion, the electronic properties of a-SiSn:H have to be vastly improved before this alloy can be considered as a viable photovoltaic material. We are currently developing new

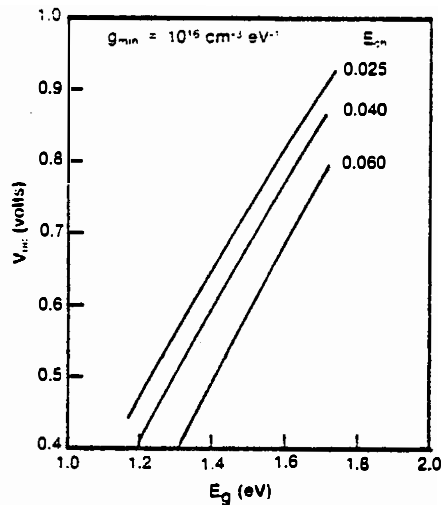

Figure 5 - Open circuit voltage (V_{oc}) is plotted as a function of E_g, for different values of E_{ch}, as defined in the text for an incident illumination of 100mW cm^{-2}.

techniques to deposit a-SiSn:H in different local bonding configurations without the complicating effects of C or Cl incorporation, and shall report on this in the near future.

Acknowledgements

The authors would like to thank Kyle Sadlon for help in measuring the electrical properties of the alloy films and Dr. Chuck Herrington for the electron microprobe data. This work is supported by DOE under Contract No. DE-AC02-83CH10093.

References

(1) Y. Kuwano, M. Ohnishi, S. Nishiwaki, T. Tsuda, T. Fukatsu, K. Enomoto, Y. Nakashima, and H. Tarui, Proceedings 16th IEEE PV Specialists Conference, (San Diego, 1982), 1338.

(2) G. Nakamura, K. Sato, and Y. Yukimoto, Proceedings 16th IEEE PV Specialists Conference, (San Diego, 1982), p. 1331.

(3) D. Hauschildt, R. Fischer, and W. Fuhs, Phys. Status. Solid B 102, (1980) 563.

(4) B. von Roedern, D.K. Paul, J. Blake, R.W. Collins, G. Moddel and William Paul, Phys. Rev. B25 (1982) 7678.

(5) D.L. Williamson, R.C. Kerns, and S.K. Deb, J. Appl. Phys. 55 (1984) 2816.

(6) A.H. Mahan, D.L. Williamson, and A. Madan, Appl. Phys. Lett. 44 (1984) 220.

(7) B. von Roedern, A.H. Mahan, R. Könenkamp, D.L. Williamson, A. Sanchez and A. Madan, Topical Conf. on Transport and Defects in Amorphous Semicond., Bloomfield Hills, MI (1984) in press.

(8) W. Paul, D.K. Paul, B. von Roedern, J. Blake, and S. Oguz, Phys. Rev. Lett. 46, (1981) 1016.

(9) G. Nakamura, K. Sato, Y. Yukimoto, and K. Shirahata, Japan J. Appl. Phys. 20 (1981) Supplem. 20-2, 227.

(10) R.L. Weisfield, J. Appl. Phys. 54 (1983) 6401.

(11) W.B. Jackson and N.M. Amer, J. Physique 42 (1981) Supplem. C-4, 293.

(12) A. Morimoto, T. Miura, M. Kumeda and T. Shimizu, Japan. J. Appl. Phys. 20 (1981) L833.

(13) A. Morimoto, T. Miura, M. Kumeda and T. Shimizu, J. Appl. Phys. 53 (1982) 7299.

(14) W.B. Jackson, Solid State Commun. 44 (1982) 477.

(15) P. Nielsen and R. Gredin, J. Vac. Sci. Tech. A 1 (1983) 583.

(16) A.H. Mahan, private communication.

(17) Y. Tawada, K. Tsuge, M. Kondo, H. Okamoto, and Y. Hamakawa, J. Appl. Phys. 53, (1982) 5273.

(18) A.A. Andreev, O.A. Golikova, F.S. Nasredinov, P.V. Nistiryuk, and P.P. Seregin, Sov. Phys. Semicond. 16, (1982) 715.

(19) R.L. Weisfield, Ph.D. Thesis, Harvard University (1983).

(20) P.B. Kirby, W. Paul, C. Lee, S. Lin, B. von Roedern, and R.L. Weisfield, Phys. Rev. B28 (1983) 3635.

(21) W.E. Spear and P.G. LeComber, Phil. Mag. 33, (1976) 935.

(22) A. Madan, W. Czubatyj, D. Adler, and M. Silver Phil. Mag. 42 (1980) 257.

(23) See, for example, N.F. Mott and E.A. Davis, Electronic Processes in Non-Crystalline Materials (Clarendon, Oxford, 1979), Chap. 7.